LIANG CHEN
XIANBIAO MAO
and
PENG WU

Non-linear dynamic support optimization method for non-uniform pressure circular tunnel considering the effect of damage

Based on non-linear Hoek-Brown criterion, a new approximate solution of deformation and plastic zone radius of circular tunnel is deduced under non-uniform pressure. In the plastic region, three different, Young's modulus attenuation models are applied to solve the plastic zone deformation. The results show that the lateral pressure coefficient (LPC), dilatancy coefficient, buried depth and Young's modulus attenuation exert important effects on the surrounding rock state. Under the influence of LPC, the radius and displacement of plastic zone show non-uniform variation; then, the maximum value of the ground response curve is gradually shifted from the side to the roof. With the burial depth and dilatancy coefficient increase, the surface displacement presents the non-linear increase characteristic. Besides, the influence of Young's modulus on the plastic zone deformation is not only related to its attenuation model, but also closely related to the surface location and LPC of surrounding rock. Based on the above research, a non-linear dynamic support optimization method for non-uniform pressure circular tunnel is proposed.

Keywords: *Elastoplastic solution; circular tunnel; non-linear Hoek-Brown criterion; lateral pressure coefficient; ground response curve*

1. Introduction

Although the plane strain problem of circular holes is relatively simple problem, it can provide effective theoretical bases for the optimization of tunnel section shape, support design and stability evaluation of surrounding rock in underground engineering. Therefore, plane strain problems have been widely applied in the tunnel excavation, shaft construction, oil extraction, coal gas penetration and other projects.

The elastic solution of a cylindrical cavity excavated in biaxial in situ stress fields was put forward as early as 1898

Messrs. Liang Chen, State Key Laboratory for Geomechanics and Deep Underground Engineering, China University of Mining & Technology, Xianbiao Mao and Peng Wu, Liang Chen, State Key Laboratory for Geomechanics and Deep Underground Engineering, China University of Mining & Technology, School of Mechanics and Civil Engineering, China University of Mining & Technology, 221116 Xuzhou, China, Correspondence addressed: Xianbiao Mao; xbmaocumt@163.com

by Kirsch. However, the plastic behaviour of the material was ignored. Later, R.Fenner firstly proposed a elastoplastic analytical solution of a circle tunnel under the uniform pressure. Then, based on the complex variable function theory or finite element method, Savin, Detournay and Zhou et al. [1-4] presented the solutions of displacement and plastic zone radius of a circular tunnel under non-uniform pressure. What is more, Zhao [5] introduced a simplified stress solution of elastic zone for weakly consolidated soft rock tunnel under asymmetry load and the accuracy of the solution was proved by experimental results and engineering cases. However, the previous studies have mostly used Mohr-Coulomb criterion. It may be unreasonable to adopt these criterion for the jointed and fractured rock masses because it easily showed obvious non-linear failure characteristics in the process of compression experiment [6]. The non-linear Hoek-Brown (H-B) yield criterion for such rock has good applicability [7-8]. In the past twenty years, many scholars have carried out a great deal of research on the distribution of surrounding rock state of circular tunnel by means of theoretical analysis and numerical simulation combined with the H-B yield criterion under uniform pressure [8-16]. However, due to the difficulty of solving, the influence of lateral pressure coefficient (LPC) on the changes of surrounding rock state was rarely considered under H-B yield criterion. So, in this paper, on the basis of certain assumptions, a new approximate closed solution of a circular tunnel excavated in the H-B rock mass under non-uniform pressure was obtained and the radius and deformation of the plastic zone was also deduced. Finally, the accuracy of the solution was also proved by comparing with the Park's solution [12].

With the increase of plastic deformation of surrounding rock, the internal cracks in the rock mass will gradually expand, and then the mechanical parameters, such as Young's modulus, H-B constants, Poisson's ratio et al, will gradually decrease. As for Young's modulus, there are mainly two ways to define the post-peak attenuation process. First, the Young's modulus could be determined by confining pressure and the minimum principal stress, which is named pressure-dependent Young's modulus (PDM) model [17-20]; Secondly, the Young's modulus attenuation model is a function associated with the plastic zone radius, that is, radius-

dependent Young's modulus (RDM) model [21-24]. In order to reflect the influence of Young's modulus attenuation on the surrounding rock state, the RDM model would be cited by this paper. Based on RDM model, three different Young's modulus attenuation models will be proposed to study the effect of Young's modulus on surrounding rock deformation.

Based on non-linear H-B criterion and certain assumptions, a new approximate closed solution of stress, deformation and plastic zone radius of surrounding rock in circular tunnel was deduced under non-uniform pressure. Meanwhile, by comparing with the Park's solution [12], the correctness of this paper is verified. And then, the effects of the LPC, the dilatancy coefficient, buried depth, Young's modulus attenuation and rock quality grade on the surrounding rock state are systematically studied. Finally, a non-linear dynamic support method for non-uniform pressure circular tunnel is proposed, which provides references for similar engineering problems.

2. Definition of the problem

As shown in Fig.1, a circular tunnel with inner radius a is excavated in a uniform, isotropic and continuous H-B rock mass. The initial vertical stress and horizontal stress at the infinite boundary are respectively σ_0 and $\lambda\sigma_0$, where λ is the lateral pressure coefficient (LPC). The inner radius a of the circular tunnel is subject to a pressure p_{in}. As the pressure p_{in} gradually decreases, the surrounding rock deformation gradually converges, and the stress state of the surrounding rock is also gradually redistributed. In the initial excavation period, the surrounding rock is in the elastic state. When the maximum and minimum principal stresses satisfy the non-linear H-B yield criterion, the stress-strain curve show

obvious stress drop characteristics and then the plastic zone develops. Eventually, the surrounding rock would achieve a stress equilibrium state with the plastic zone radius R_p under the effect of the pressure p_{in}. Meanwhile, the rock mass mechanical parameters, such as Young's modulus, H-B constants, Poisson's ratio et al, will also gradually decrease and then reach the residual value.

In this paper, the non-linear H-B criterion as the rock mass yield condition can be expressed as [8,10-13,15]:

$$\sigma_1 = \sigma_3 + \sqrt{m_b\sigma_c\sigma_3 + s\sigma_c^2} \qquad \text{... (1)}$$

Where σ_1 and σ_3 represent respectively the maximum principal stress and the minimum principal stress; σ_c represents the initial uniaxial compressive strength; parameters m_b and s represent the rock material constants determined by H-B criterion.

For the plane strain problem, when the support pressure meets the conditions $p_{in} << [\sigma_0, \lambda\sigma_0]_{min}$, the radial stress ($\sigma_r$) and tangential stress($\sigma_\theta$) in generally are the minimum principal stress and the maximum principal stress respectively [5]. Therefore, Equation (1) can be expressed as:

$$\sigma_\theta = \sigma_r + \sqrt{m_b\sigma_c^{Peak}\sigma_r + s\sigma_c^{Peak2}} \quad \text{for intact rock mass} \quad (2a)$$

$$\sigma_\theta = \sigma_r + \sqrt{m_{br}\sigma_{cr}^R\sigma_r + s_r\sigma_{cr}^{R2}} \quad \text{for residual rock mass} \quad (2b)$$

Where σ_c^{Peak} represents the initial uniaxial compressive strength of rock mass; σ_{cr}^R represents the residual compressive strength; m_{br} and s_r represent the H-B rock mass residual constants. $\sigma_c^{Peak} = 2c \cos \varphi/(1-\sin\varphi)$, $\sigma_{cr}^R = 2c \cos \varphi_r /(1-\sin\varphi)$. c and c_r represent the initial and residual cohesion respectively, φ and φ_r represent the initial and
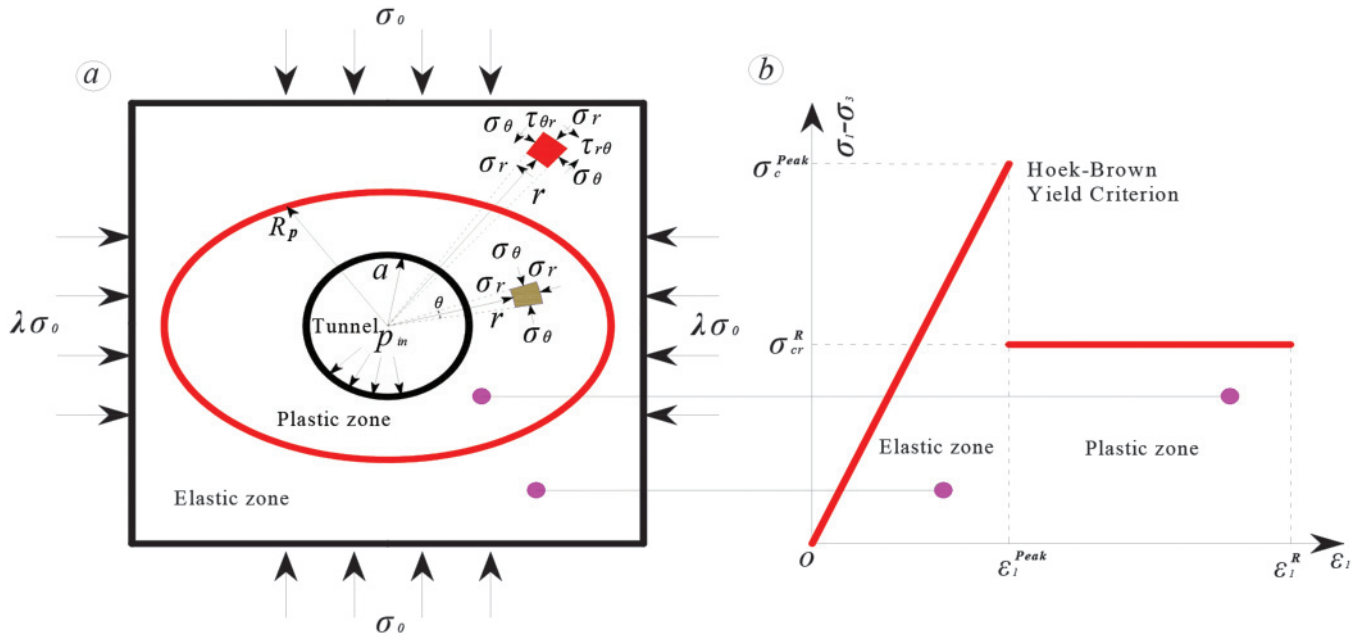

Fig.1 Mechanical model of a deep circular tunnel.

residual internal friction angles of rock mass.

When the surrounding rock enters the plastic zone, its mechanical behaviour is closely related to the rock damage degree. The higher the rock is damaged, the greater the deformation becomes. Generally, the Young's modulus attenuation could be used to indicate the damage degree of surrounding rock. In this paper, based on the radius-dependent Young's modulus (RDM) model, three different Young's modulus attenuation model will be proposed to calculate the deformation of plastic zone.

• Case 1: Assume the Young's modulus of plastic zone equals to the initial value E, which means neglecting the influence of Young's modulus attenuation on the state of surrounding rock. So, it can be expressed as:

$$E(r) = E \qquad \qquad ... (3)$$

Where $E(r)$ represents the Young's modulus of plastic zone; E represents the initial rock mass Young's modulus.

• Case 2: Young's modulus along with the radius direction of plastic zone presents the power function attenuation characteristics. Considering the continuity condition of the Young's modulus attenuation, $E(r)_{r=Rp} = E$, $E(r)_{r=a} = E_r$, then the Young's modulus at any point of plastic zone can be expressed as:

$$E(r) = E_r(r/a)^\alpha \qquad \qquad ... (4)$$

Where $\alpha = \log(E/E_r)/\log(R_p/a)$, Er represents residual Young's modulus.

• Case 3: Assume the Young's modulus of plastic zone is equal to a certain residual value E_r, the Young's modulus of the plastic zone can be expressed as:

$$E(r) = E_r \qquad \qquad ... (5)$$

The Eq. (4) shows that the Young's modulus attenuation is not only related to the initial and residual value, but also closely related to the radius of plastic zone. Compared to the solution presented by Zhang and Ewy [23, 24], the solution of this paper is obtained under non-uniform pressure. Therefore, the radius (R_p) of plastic zone is constantly changing around the surrounding rock, and then the Young's modulus attenuation degree is also different, which exerts an important influence on the plastic zone displacement and support scheme design.

3. Closed solutions of circular tunnels

3.1 BASIC EQUATION

Considering the assumptions condition, the equilibrium equations of plastic zone for the plane strain problem can be written as:

$$d\sigma_r/dr + (\sigma_r - \sigma_\theta)/r = 0 \qquad \qquad ... (6)$$

The geometric equation of this problem can be denoted as:

$$\varepsilon_r = \frac{du}{dr}; \varepsilon_\theta = \frac{u}{r} \qquad \qquad ... (7)$$

Where ε_r and ε_θ respectively represent the radial strain and tangential strain; u represents the radial displacement of surrounding rock. Based on the small deformation assumption, the elastic strain part of plastic zone satisfies Hoek's law as:

$$\begin{cases} \varepsilon_r = \dfrac{1+\nu}{E}[(1-\nu)(\sigma_r - \sigma_0) - \nu(\sigma_\theta - \sigma_0)] \\ \varepsilon_\theta = \dfrac{1+\nu}{E}[(1-\nu)(\sigma_\theta - \sigma_0) - \nu(\sigma_r - \sigma_0)] \end{cases} \qquad ... (8)$$

where, ν represents initial poisson ratio.

3.2 STRESS AND DEFORMATION SOLUTION OF ELASTIC ZONE

Based on the elasticity theory and Kirsch's solution [25], the approximate stress expression of elastic zone under non-uniform pressure can be obtained as Eq.(9a). The result is similar to Zhao's solution [5].

$$\begin{cases} \sigma_{re} = \dfrac{(1+\lambda)\sigma_0}{2}(1 - \dfrac{R_p^2}{r^2}) + p_y \dfrac{R_p^2}{r^2} - \dfrac{(1-\lambda)\sigma_0}{2}(1 - 4\dfrac{R_p^2}{r^2} + 3\dfrac{R_p^4}{r^4})\cos 2\theta \\ \sigma_{\theta e} = \dfrac{(1+\lambda)\sigma_0}{2}(1 + \dfrac{R_p^2}{r^2}) - p_y \dfrac{R_p^2}{r^2} + \dfrac{(1-\lambda)\sigma_0}{2}(1 + 3\dfrac{R_p^4}{r^4})\cos 2\theta \end{cases} \qquad (9a)$$

Where, p_y is the radial contact stress at the interface between elastic and plastic zone. When $\lambda = 1$, Eq.(9a) will be transformed into the stress expression under uniform pressure which is the same as Park's solution [11]. In other words, Park's solution is only a special case of this paper.

$$\begin{cases} \sigma_{re} = \sigma_0 - (\sigma_0 - p_y)\dfrac{R_p^2}{r^2} \\ \sigma_{\theta e} = \sigma_0 + (\sigma_0 - p_y)\dfrac{R_p^2}{r^2} \end{cases} \qquad ... (9b)$$

Substituting Eqs.(7) and (9a) into Eq.(8), the displacement expression of elastic zone can be obtained by considering stress instantaneous release.

$$u_{re} = \dfrac{(1+\nu)r}{E}\{(1-\lambda)\nu\sigma_0 + [\dfrac{(1+\lambda)\sigma_0}{2} - 2(1-\lambda) \\ \nu\sigma_0 \cos 2\theta - p_y]\dfrac{R_p^2}{r^2} + \dfrac{3(1-\lambda)\sigma_0}{2}\dfrac{R_p^4}{r^4}\} \qquad ... (10)$$

When $r = R_p$, the displacement expression at the interface between elastic and plastic zone can be deduced:

$$u_{R_p} = \dfrac{(1+\nu)R_p}{E}\{(1-\lambda)\nu\sigma_0 + [\dfrac{(1+\lambda)\sigma_0}{2} - 2(1-\lambda) \\ \nu\sigma_0 \cos 2\theta - p_y] + \dfrac{3(1-\lambda)\sigma_0}{2}\} \qquad ... (11)$$

At the elastoplastic contact surface, the surrounding rock is in the critical yield state, so the tangential and radial stresses meet the non-linear H-B yield criterion at the peak point. Substituting Eqs (9a) into Eq (2a), the radial contact stress p_y under non-uniform pressure firstly can be obtained:

$$p_{y1} = \frac{1}{8}\{4[(1+\lambda)\sigma_0 + 2(1-\lambda)\sigma_0 \cos 2\theta] + m_b \sigma_c^{Peak}\}$$
$$-\frac{1}{8}\sqrt{\{8[(1+\lambda)\sigma_0 + 2(1-\lambda)\sigma_0 \cos 2\theta] + m_b \sigma_c^{Peak}\} m_b \sigma_c^{Peak} + 16 s\sigma_c^{Peak\,2}} \quad (12)$$

When $\lambda=1$, the radial contact stress under uniform pressure can be obtained:

$$p_{y2} = \sigma_0 + \frac{1}{8}m_b\sigma_c^{Peak} - \frac{1}{8}\sqrt{(16\sigma_0 + m_b\sigma_c^{Peak})m_b\sigma_c^{Peak} + 16s\sigma_c^{Peak2}} \quad (13)$$

Compared to Eq (13), Eq (12) is obtained under the non-uniform pressure. So, the radial contact stress (p_y) changes with the rotation angle (θ), which shows that the critical supporting resistance at each point of the tunnel surface is different. And this phenomenon has important influences on the range of plastic zone, deformation and the design of the supporting structure.

3.3 STRESS AND DEFORMATION OF THE PLASTIC SONE

3.3.1 Stress and radius solution of the plastic zone

Based on the assumption conditions, the stress of plastic zone should satisfy the post-peak H-B yield criterion and equilibrium equations. Therefore, substituting Eq.(2b) in to Eq.(6), the stress of plastic zone can be obtained by considering boundary condition $\sigma_{rp} = p_{in}$ at $r=a$.

$$\begin{cases} \sigma_{rp} = H_1 \ln(\frac{r}{a}) + H_2 \ln^2(\frac{r}{a}) + p_{in} \\ \sigma_{\theta p} = (H_1 + 2H_2)\ln(\frac{r}{a}) + H_2 \ln^2(\frac{r}{a}) + H_1 + p_{in} \end{cases} \quad (14)$$

where $H_1 = (m_{br}\sigma_{cr}^R p_{in} + s_r\sigma_{cr}^{R2})^{1/2}$; $H_2 = \frac{m_{br}\sigma_{cr}^R}{4}$.

From Eqs.(9a) and (9b),the radius of plastic zone should be firstly determined in order to obtain the stress closed analytical solution of surrounding rock. Considering the stress boundary conditions $(\sigma_{rp})_{r=Rp} = p_{yi}$ at $r=R_p$, the radius of plastic zone under non-uniform pressure can be deduced by combining Eqs.(12) and (14):

$$R_{p1} = a\exp\left[\frac{-H_1 + \sqrt{(H_1)^2 - 4H_2(p_{in} - p_{y1})}}{2H_2}\right] \quad (15)$$

When $\lambda=1$, the radius of plastic zone under uniform pressure is obtained by combining Eqs.(13) and (14):

$$R_{p2} = a\exp\left[\frac{-H_1 + \sqrt{(H_1)^2 - 4H_2(p_{in} - p_{y2})}}{2H_2}\right] \quad (16)$$

3.3.2 Displacement solution of plastic zone

If the tangential strain and radial strain in plastic zone are composed of elastic strain and plastic strain, the total strain can be expressed as:

$$\begin{cases} \varepsilon_{rp} = \varepsilon_r^e + \varepsilon_r^p \\ \varepsilon_{\theta p} = \varepsilon_\theta^e + \varepsilon_\theta^p \end{cases} \quad (17)$$

Where, ε_r^p and ε_θ^p represent the radial strain and tangential strain in plastic zone respectively.

In general, the deformation of rock materials in plastic zone satisfying the non-associated flow law can be determined by the M-C plastic potential function which can be expressed as follows:

$$f(\sigma_\theta, \sigma_r) = \varepsilon_\theta - \beta_r\sigma_r \qquad \dots (18)$$

Where, $\beta_r = (1+\sin\psi)$ $(1-\sin\psi)$, ψ represent dilatancy angle of rock mass.

According to the plastic potential theory, the plastic tangential strain ε_θ^p and radial strain ε_r^p can be expressed as:

$$\varepsilon_\theta^p = \lambda_p \frac{\partial f}{\partial \sigma_{\theta p}}, \quad \varepsilon_r^p = \lambda_p \frac{\partial f}{\partial \sigma_{rp}} \qquad \dots (19)$$

Where λ_p represent the parameters relevant to the plastic strain.

Substituting Eq.(18) in to Eq.(19), the relationship between plastic tangential strain and radial strain can be obtained:

$$\varepsilon_r^p + \beta_r\varepsilon_\theta^p = 0 \qquad \dots (20)$$

Substituting Eqs. (7) and (20) in to Eq. (17), the differential equation of radial displacement in plastic zone can be obtained:

$$\frac{du_{rp}}{dr} + \beta_r \frac{u_{rp}}{r} = f(r) \qquad \dots (21)$$

Where, $f(r) = \varepsilon_r^e + \beta_r \varepsilon_\theta^e$ Solving Eq (21) and considering displacement continuous condition

$(u_{rp})_{r=R_p} = u_{R_p}$ at $r=R_p$, the radial displacement in plastic zone can be deduced:

$$u_{rp} = \frac{1}{r^{\beta_r}}\int_{R_p}^r f(r)r^{\beta_r}dr + u_{R_p}(\frac{R_p}{r})^{\beta_r} \qquad \dots (22)$$

Eq. (22) shows that the displacement is closely related to the expression of elastic strain in plastic zone. The elastic strain in plastic zone satisfies the generalized Hook's law. Considering the attenuation of Young's modulus, the elastic strain in plastic zone at any point should satisfy the following equation.

$$\begin{cases} \varepsilon_\theta^e = \frac{1+v_r}{E^j(r)}[(1-v_r)(\sigma_{\theta p} - \sigma_0) - v_r(\sigma_{rp} - \sigma_0)] \\ \varepsilon_r^e = \frac{1+v_r}{E^j(r)}[(1-v_r)(\sigma_{rp} - \sigma_0) - v_r(\sigma_{\theta p} - \sigma_0)] \end{cases} \quad (23)$$

Where, "$E^j(r)$" represents different models of the Young's modulus attenuation respectively, such as Case 1, Case 2 and Case 3. Substituting Eq. (23) in to function $f(r)$, the specific expressions of the function $f(r)$ can be obtained:

$$f(r) = \frac{1+v_r}{E^j(r)}[(1-v_r-v_r\beta_r)\sigma_{rp} + (\beta_r - v_r\beta_r - v_r)\sigma_{\theta p} + (2v_r-1)(1+\beta_r)\sigma_0] \qquad \dots (24)$$

Substituting Eq. (14) in to Eq. (24), the function $f(r)$ can be obtained under the non-uniform pressure:

$$f(r) = \frac{1+v_r}{E^j(r)}[\delta_1 \ln^2(\frac{r}{a}) + \delta_2 \ln(\frac{r}{a}) + \delta_3] \qquad \ldots (25)$$

where, $\delta_1 = (1+\beta_r)(1-2v_r)H_2$, $\delta_2 = (1+\beta_r)(1-2v_r)H_1 + 2(\beta_r - v_r\beta_r - v_r)H_2$, $\delta_3 = (1+\beta_r)(1-2v_r)(p_{in} - \sigma_0) + (\beta_r - v_r\beta_r - v_r)H_1$.

For Case 1, substituting Eqs.(3) and (25) into Eq.(22), the displacement of plastic zone without considering Young's modulus attenuation can be deduced:

$$u_{rp}^{case1} = \frac{1}{2Gr^{\beta_r}}[\delta_1 f_1(r) + \delta_2 f_2(r) + \delta_3 f_3(r) - \delta_1 f_1(R_p) \\ - \delta_2 f_2(R_p) - \delta_3 f_3(R_p) + 2Gu_{R_p}R_p^{\beta_r}] \qquad \ldots (26)$$

where, $G = E/[2(1+v_r)]$,

$$f_1(r) = \frac{r^{1+\beta_r}}{1+\beta_r}[\ln^2(\frac{r}{a}) - \frac{2}{1+\beta_r}\ln(\frac{r}{a}) + \frac{2}{(1+\beta_r)^2}],$$

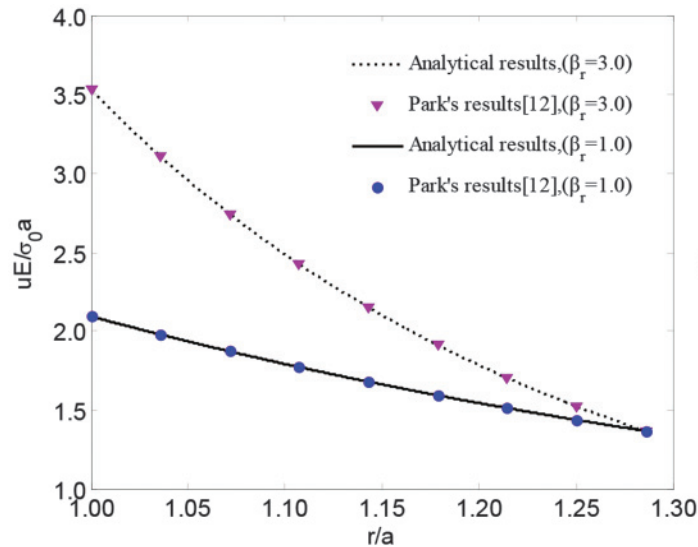$$f_2(r) = \frac{r^{1+\beta_r}}{1+\beta_r}[\ln(\frac{r}{a}) - \frac{1}{1+\beta_r}], f_3(r) = \frac{r^{1+\beta_r}}{1+\beta_r}.$$

For Case 2, substituting Eqs.(4) and (25) into Eq.(22), the displacement of plastic zone can be obtained by considering Young's modulus power function attenuation.

$$u_{rp}^{case3} = \frac{a^\alpha}{2G_r r^{\beta_r}}[\delta_1 f_1(r) + \delta_2 f_2(r) + \delta_3 f_3(r) - \delta_1 f_1(R_p) \\ - \delta_2 f_2(R_p) - \delta_3 f_3(R_p) + 2G_r u_{R_p}a^{-\alpha}R_p^{\beta_r}] \qquad (27)$$

where, $f_1(r) = \frac{r^{1+\beta_r-\alpha}}{1+\beta_r-\alpha}[\ln^2(\frac{r}{a}) - \frac{2}{1+\beta_r-\alpha}\ln(\frac{r}{a}) + \frac{2}{(1+\beta_r-\alpha)^2}],$

$$f_2(r) = \frac{r^{1+\beta_r-\alpha}}{1+\beta_r-\alpha}[\ln(\frac{r}{a}) - \frac{1}{1+\beta_r-\alpha}], f_3(r) = \frac{r^{1+\beta_r-\alpha}}{1+\beta_r-\alpha}$$

For Case 3, the displacement expression form of plastic zone is same as the Eq.(26). Substituting Eq. (5) and (25) into Eq.(22), the displacement of plastic zone can be obtained as well when the parameter G in the Eq. (26) is transformed into G_r. Where $G_r = E_r/[2(1+v_r)]$.

4. Example analysis

4.1 COMPARATIVE ANALYSIS OF EXAMPLES

Compared to the traditional closed-form solution, this paper considers the influence of the LPC on the change of the surrounding rock state under non-linear H-B criterion. When $\lambda=1$, the solution will be transformed into the traditional solution under uniform pressure. In response to this problem, Park et al. [12] also conducted some studies without considering the impact of LPC, post-peak Young's modulus attenuation, Poisson's ratio and compressive strength, which is inconsistent with the actual project. That is, when the parameters $\lambda=1$, $E=E_r$, $v=v_r$, $\sigma_c^{Peak} = \sigma_c^R$, the solution of this paper is the same with Park's solution. In this case, the radial contact stress p_y and the radius of plastic zone R_p can be determined by Eq (12) or (13) and Eq (15) or (16) respectively. In order to verify the accuracy of the results, the authors compare them with Park's solution.

The comparison between the solution in this paper and the Park's solution is shown in Fig.2. When $\lambda = 1$, $v=v_r$, $\sigma_c^{Peak} = \sigma_c^R$, this paper's solution is the same with Park's solution. Therefore, Park's solution is a particular case of this paper. In other words, the solution of this paper has a wider applicability.

4.2 PARAMETER ANALYSIS

The range and deformation of plastic zone are the important basis for evaluating the stability of the surrounding rock and the reliability of the supporting design. From the Eqs
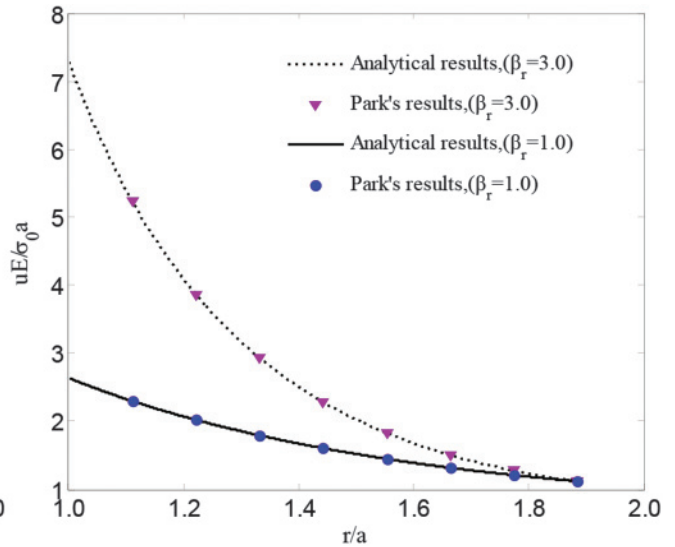

Fig.2 The comparison of this paper's solution with the Park's solution. (parameter values: $\lambda=1$, $v=v_r$ $\sigma_c=\sigma_c^{Peak}=\sigma_c^R$ (a) Radial displacement with hard rock parameters (b) Radial displacement with soft rock parameters.

TABLE 1 GEOMETRICAL AND PHYSICAL PARAMETERS OF CIRCULAR TUNNEL

Parameters	Set 1-(Park[12])	
	Hard rock	Soft rock
Radius of opening, a(m)	4	5
Initial stress, σ_0(MPa)	108	30
Internal pressure, p_{in}(MPa)	0	5
Young's modulus, E(MPa)	40000	5500
Poisson's ratio, ν	0.2	0.25
Shear modulus, G(MPa)	16667	2200
H-B		
m_b	7.5	1.7
s	0.1	0.0039
m_{br}	1.0	1.0
s_r	0.01	0
σ_c(MPa)	300	30

(9a), (15), (26) and (27), the state of surrounding rock is not only related to the parameters of the surrounding rock, but also closely related to the LPC. Table 2 shows the parameters and the H-B constant for the different quality grades rock mass.

4.2.1 Effects of the LPC on the plastic zone radius

The plastic zone radius R_p and radial contact stress p_y under non-uniform pressure can be respectively calculated by Eqs.(15) and (12). Fig.3 shows the effects of the LPC on the radius of plastic zone. When $\lambda \neq 1$, the range of plastic zone shows the non-uniform change characteristics along its circumference. With the increasing LPC, the range of the plastic zone in the side wall decreases gradually, while that in the roof or floor increases gradually. For example, for the quality grade-C rock mass, when the λ is changed from 0.7 to 1.6, the radius of plastic zone (R_p/a) decreases from 2.81 to 1.39, whereas the roof increases from 1.05 to 7.03. Besides, when $0<\lambda<1$, the ranges of plastic zone in two side are larger

than those in the roof or floor. When $\lambda>1$, the results are on the contrary. The above analysis shows that, when $0<\lambda<1$ changes to $\lambda > 1$, the key part of the first failure of the tunnel is gradually transferred from two sides to the roof and floor, so the support design of the non-uniform pressure tunnel should take full account of the influence of LPC on the state of surrounding rock.

4.2.2 Effect of LPC on the surface displacement of surrounding rock

The surface displacement of the surrounding rock under non-uniform pressure can be calculated by Eqs (26) or (27). Fig.4 shows that the LPC has an important effect on the surface displacement. With the increasing LPC, surface displacement gradually decreases at two sides of tunnel, while increases at the roof and floor. For example, when the λ is changed from 0.7 to 0.9~1.1, the surface displacement of the side wall (0°) is reduced by 38mm ~ 79mm, with a decrease rate of 35.19% ~ 43.89%, while the roof and floor (90°) displacement increases by 30mm ~ 43mm, with an increasing rate 35.29% ~ 50.59%. Meanwhile, when $0<\lambda<1$, the maximum surface displacement of the tunnel is located in the side walls, and vice versa.

As shown in Fig.4 and Table 4, we can conclude that the change of inner pressure also has important influences on the deformation of surrounding rock. With the increasing inner pressure, the surface displacement of the tunnel is reduced in different degrees. For example, when $\lambda=0.9$ and the inner pressure p_{in} changes from 0MPa to 5MPa, the surface displacement of the side wall (0°), spandrel (45°) and roof (90°) are reduced by 90mm, 83mm and 75mm respectively, with a decreasing rate of 63.38%, 64.34% and 65.22%. So, we can conclude that improving the support pressure can effectively solve the problem of non-linear large deformation in deep tunnel.

TABLE 2: PARAMETERS AND H-B CONSTANT OF THE DIFFERENT QUALITY GRADES ROCK MASS

	Quality grades	Set2-H-B rock mass constant				σ_c^{Peak} /(MPa)	σ_c^R /(MPa)	E /(GPa)	E_r /(GPa)	ν	β_r
		s	s_r	m_b	m_{br}						
A	Very good[8]	0.062	0.0002	10.2	1.27	150	150	42	10	0.2	1.5
B	Average[8]	0.0039	0	2.01	0.34	80	80	9	5	0.25	1.15
C	Very poor[8]	0.0004	0.0004	0.657	0.657	20	20	1.4	1.4	0.3	1.0
D	Very poor[16]	0.0039	0.0019	1.7	0.85	30	25	5.7	5.7	0.3	1.0

TABLE 3: RADIUS OF PLASTIC ZONE WITH DIFFERENT LPC (R_p/a)

λ	Quality grade-(A)			Quality grade -(B)			Quality grade -(C)			Quality grade -(D)		
	0°	45°	90°	0°	45°	90°	0°	45°	90°	0°	45°	90°
0.7	2.02	1.70	1.41	1.62	1.23	0.00	2.81	1.80	1.05	2.50	1.78	1.19
1.0	1.86	1.86	1.86	1.42	1.42	1.42	2.27	2.27	2.27	2.12	2.12	2.12
1.3	1.70	2.02	2.35	1.23	1.62	2.07	1.80	2.81	4.17	1.78	2.50	3.37
1.6	1.56	2.18	2.91	1.06	1.84	2.90	1.39	3.44	7.03	1.47	2.91	5.04

4.2.3 Effects of burial depth on the state of surrounding rock

As shown in Fig.5, burial depth has an important effect on the plastic zone radius and the surface displacement. With the increasing burial depth, the surface displacement and the radius of the plastic zone also gradually increase. For example, for the quality grade-B rock mass, the surface displacement of the surrounding rock increases by 8mm, and the radius of the plastic zone increases by 750mm when σ_0 changes from

20MPa to 24MPa. Meanwhile, compared to the better quality rock mass, the worse quality rock have more sensitive to buried depth.

4.2.4 Effects of dilatancy coefficient on surface displacement of surrounding rock

The effect of the dilatancy coefficient on the surface displacement is shown in Fig.6. The dilatancy coefficient has

Fig.3 Effects of the LPC on the plastic zone radius. (a) (Grades-A rock mass parameters: parameters: parameters: σ_0=108MPa, a=4m, p_{in}=0MPa). (b) (Grades-B rock mass parameters: σ_0=30MPa, a=5m, p_{in}=5MPa). (c) (Grades-C rock mass parameters: σ_0=30MPa, a=5m, p_{in}=10MPa). (d) (Grades-D rock mass parameters: σ_0=30MPa, a=5m, p_{in}=5MPa).

TABLE 4: THE SURFACE DISPLACEMENT OF SURROUNDING ROCK UNDER DIFFERENT LPC (U0/M)

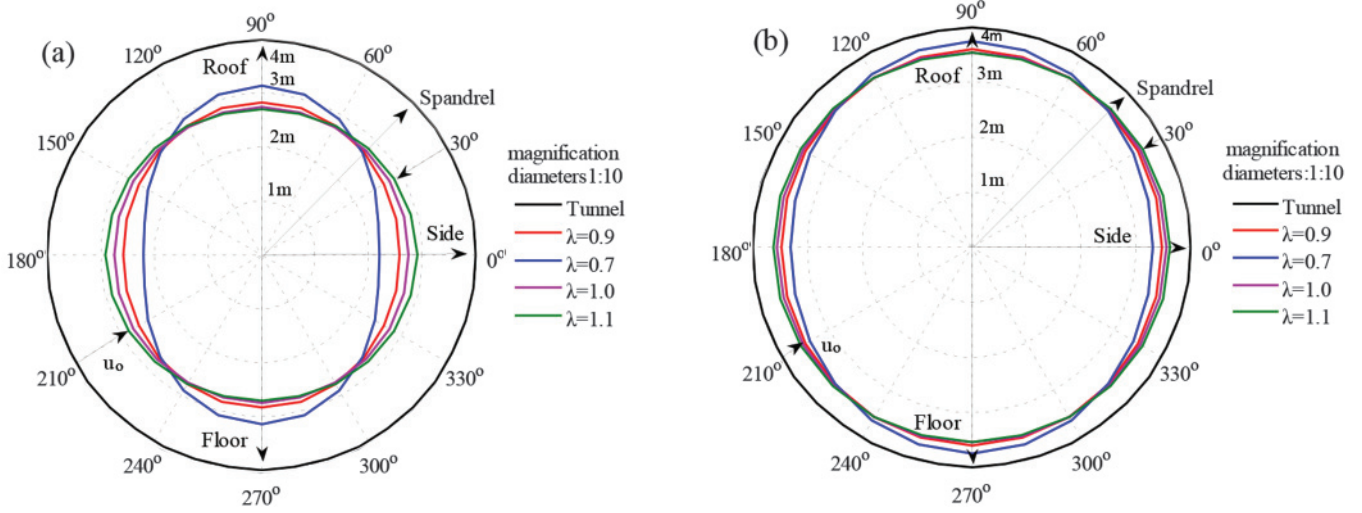| λ	Quality grade-A rock mass-(a)						Grades-A rock mass -(b)					
	0°	30°	45°	60°	75°	90°	0°	30°	45°	60°	75°	90°
0.7	0.180	0.156	0.132	0.108	0.091	0.085	0.070	0.059	0.048	0.036	0.028	0.026
0.9	0.142	0.135	0.129	0.122	0.117	0.115	0.052	0.049	0.046	0.043	0.041	0.040
1.0	0.125	0.125	0.125	0.125	0.125	0.125	0.044	0.044	0.044	0.044	0.044	0.044
1.1	0.109	0.115	0.119	0.124	0.127	0.128	0.037	0.039	0.042	0.044	0.045	0.046

Fig.4 Effect of LPC on surface displacement of surrounding rock. (a)(Grades-A rock mass parameters: $\sigma_0=108$MPa, $a=4$m, $p_{in}=0$MPa). (b) (Grades-A rock mass parameters: $\sigma_0=108$MPa, $a=4$m, $p_{in}=5$MPa)
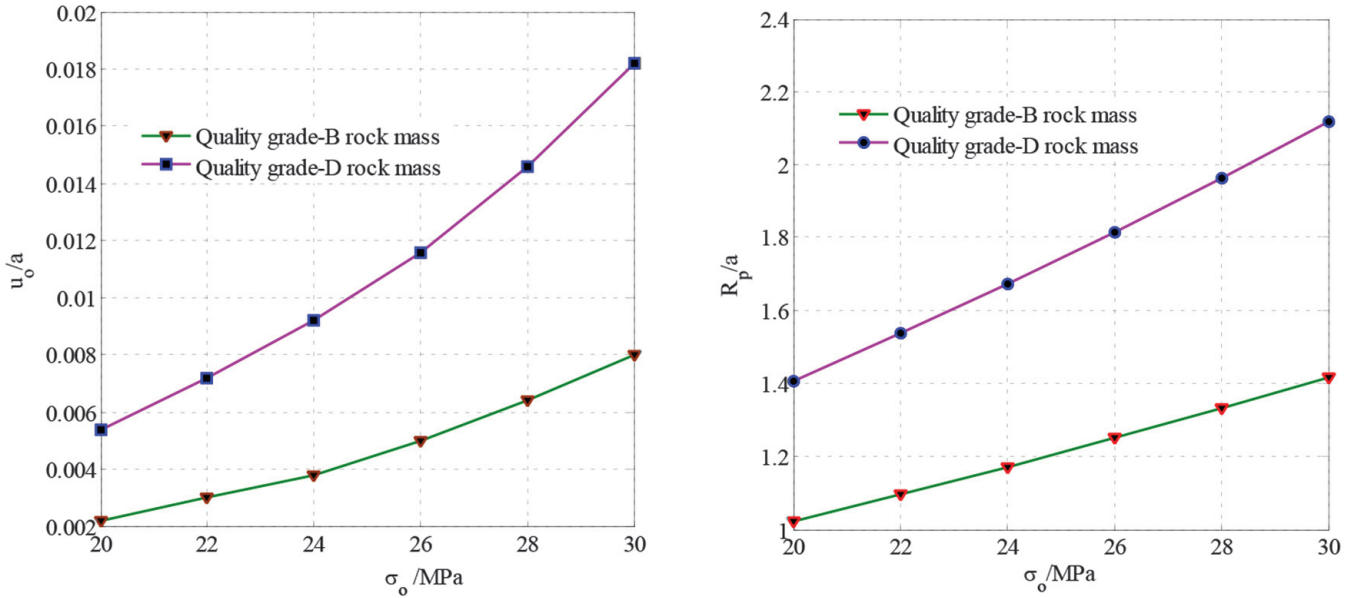

Fig.5 Effect of burial depth on the range and surface displacement of surrounding rock; (parameters: $a=5$m, $p_{in}=5$MPa, $\lambda=1.0$)

remarkable effects on the surface displacement of surrounding rock. With the increasing dilatancy coefficient, the surface displacement also gradually increases. However, compared to the better quality rock mass, the dilatancy coefficient has more significant effects on the inferior rock mass. For example, when β_r changes from 1.0 to 1.4~1.8, the surface displacement of quality grade-D rock mass increases by 25mm~58mm, while quality grade-B surface displacement increases by only 5mm~10mm. Therefore, the effects of the dilatancy coefficient on the state of the surrounding rock should be taken into full consideration in the process of the support design, especially the tunnel excavated in the soft and broken surrounding rock.

4.2.5 Effect of LPC on the ground-support response curve

The ground response curve under different LPC can be easily obtained, as shown in Fig.7. The effect of the LPC on the response curve can be summarized into two aspects as follows:

- The change characteristic of the ground response curve is closely related to the surface position of the circular tunnel. With the increasing LPC, the maximum value position of the ground response curve is gradually transferred from the side walls (0º) to the roof (90º), whose changes are consistent with the influence of the LPC on the deformation of the surrounding rock.
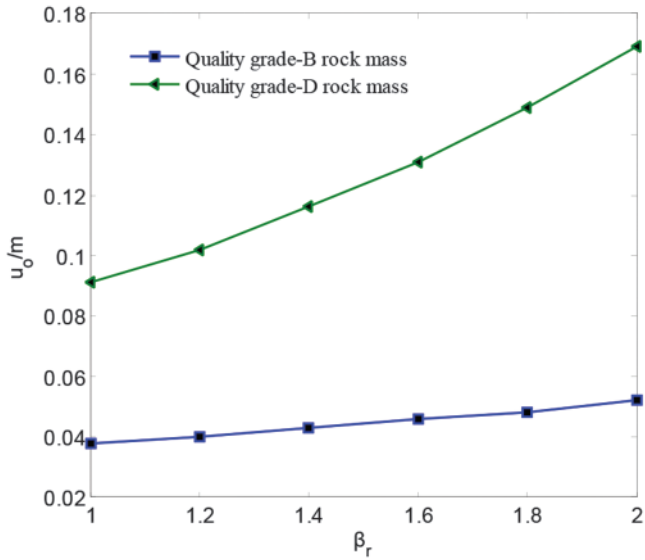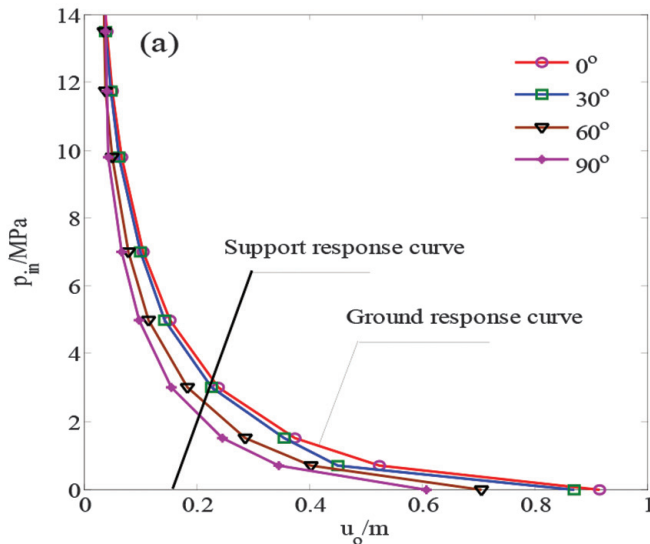
Fig.6 Effect of dilatancy coefficient on surface displacement of surrounding rock. Parameter values (Quality grade-B and D rock mass σ_0=30MPa, a=5m, p_{in}=5MPa, λ=1.0)

- The optimal support time of the surrounding rock around the circumference gradually changes with the change of the LPC. When $0<\lambda<1$, the deformation of surrounding rock under the certain inner pressure pin meets the following relations: side wall (0º) > the roof (90º). When $\lambda>1$, the opposite is true.

Table 5 illustrates the critical inner pressure p_y of different position when the surrounding rock begins to enter plastic state. When $p_{in} < p_y$, it indicates that the surrounding rock has entered the plastic state, and the ground response curve can be obtained by the Eq. (26) or (27). When $p_{in} > p_y$, the surrounding rock is still in the elastic state and the ground response curve can be obtained from Eq.(10). As shown by the above analysis, the influence of the LPC should be taken

into full consideration for the design of the primary support and the reinforced support should be carried out in the key parts to prevent rock instability.

4.3 EFFECTS OF YOUNG'S MODULUS ON THE STATE OF SURROUNDING ROCK

4.3.1 Effect of Young's modulus attenuation on the deformation of plastic zone

The effect of Young's modulus attenuation on the displacement of plastic zone is shown in Fig.8.

- It can be seen that the radial displacement of plastic zone is closely related to the selection of the Young's modulus attenuation model. Compared to the case 1, case 3 has the greatest effect on the radius displacement of plastic zone. Case 2 is the second. For example, when λ=0.7, θ=0°, compared to Case 1, the surface displacement of Case 2 and Case 3 increases by 9mm and 24mm with an increasing rate of 13.24% and 35.30% respectively.

- Meanwhile, the influence of Young's modulus attenuation on the displacement of plastic zone is closely related to the LPC. For Case 2 and Case 3, when $\theta = 60°$ and λ=0.7, the surface displacement of surrounding rock are 41 mm and 47 mm respectively. However, when $\theta = 60°$ and λ=1.1, the value significantly increases 1.049 times and 1.234 times than λ=0.7 respectively.

- Finally, the influence of Young's modulus attenuation on the deformation of the plastic zone is also closely related to the selection of the spatial location of the surrounding rock. For example, when $\lambda = 1.1$ and $\theta = 0°$, for Case 1, Case 2 and Case 3, the surface displacement of surrounding rock are 30mm, 37mm and 49mm respectively. However, when λ=1.1 and $\theta = 60°$, the value significantly increases 1.133 times, 1.162 times and 1.184 times than θ=0° respectively.

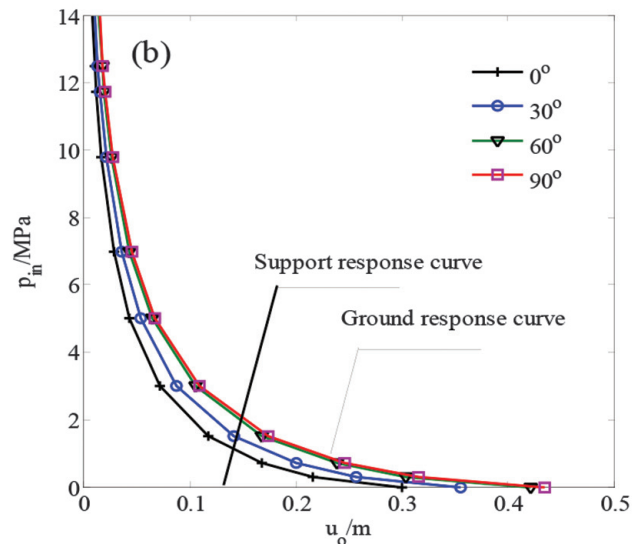Fig.7 Effect of LPC on the ground-support response curves. (Grade-D rock mass parameter: σ_0=30MPa, a=5m), (a): λ=0.8, (b) λ=1.1
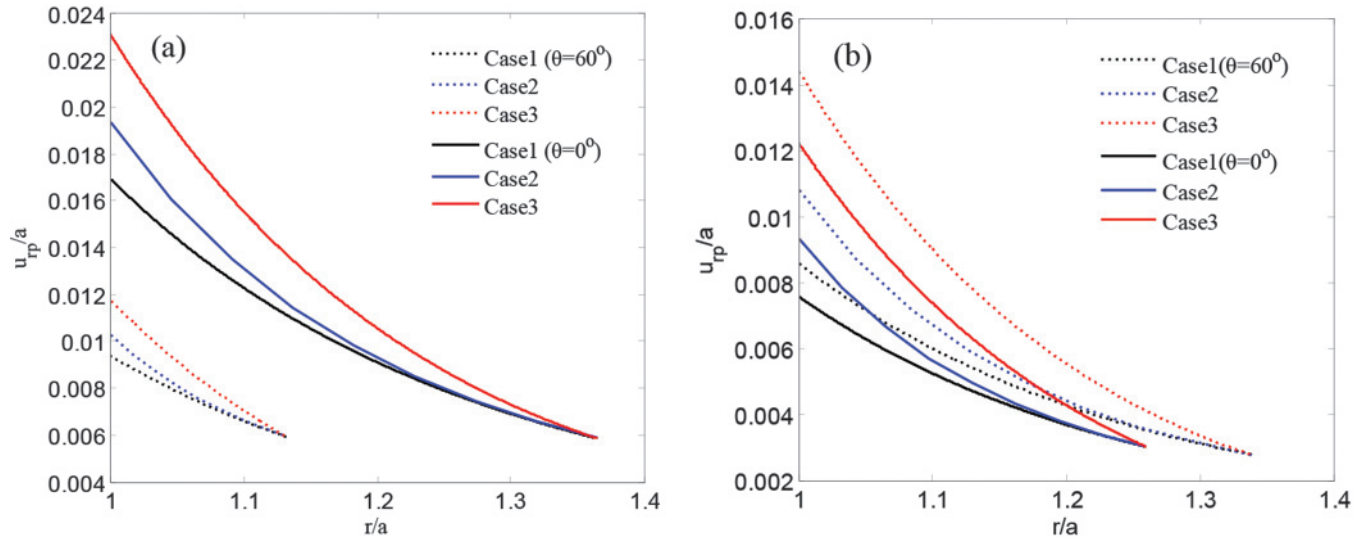
Fig.8 Effect of Young's modulus attenuation on the displacement of plastic zone. (Parameter value: Set 1– Hard rock, $v=v_r=0.2$, $\sigma_c^{Peak} = \sigma_c^R$ = 300MPa, $\beta_r=3.0$), (a) $\lambda=0.7$; (b) $\lambda=1.1$

TABLE 5: CRITICAL INNER PRESSURE p_y AT THE INTERFACE BETWEEN ELASTIC AND PLASTIC ZONE (/MPA)

λ	0°	30°	60°	90°
	/Side	/Spandrel	/Spandrel	/Roof
$\lambda=0.8$	17.875	15.783	11.733	9.789
$\lambda=1.1$	14.753	15.783	17.875	18.934

TABLE 6: SURFACE DISPLACEMENT OF SURROUNDING ROCK IN DIFFERENT CASES (u_0/m)

LPC	angle	Case1	Case2	Case3
$\lambda=0.7$	0°	0.068	0.077	0.092
	60°	0.038	0.041	0.047
$\lambda=1.1$	0°	0.030	0.037	0.049
	60°	0.034	0.043	0.058

4.3.2 Effects of Young's modulus attenuation on ground response curve.

The ground and support response curves are shown in Fig.9 in different cases of Young's modulus attenuation. It shows that when the Young's modulus attenuation is ignored (case 1), the deformation of the surrounding rock and support force will be underestimated; however, when a residual value of Young's modulus is assumed in the plastic zone (case 3), the deformation of the surrounding rock and support force will be overestimated. So, The Young's modulus power function attenuation model (case 2) seems to give more reasonable results, and is recommended for design of support parameters and stability analysis of surrounding rock in circular tunnel.
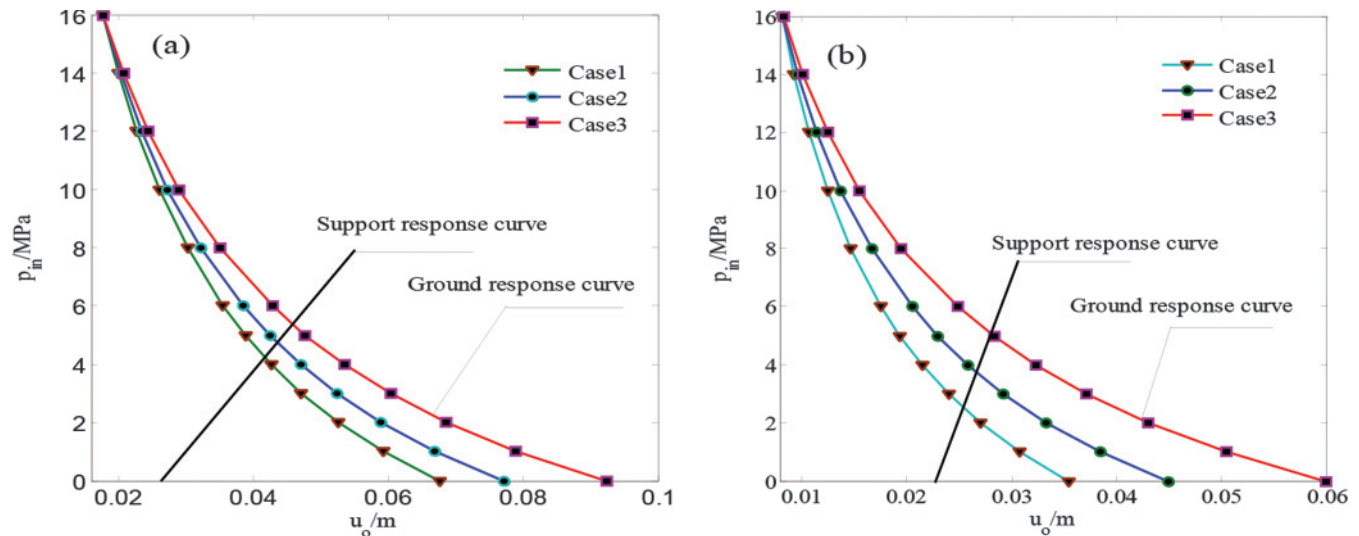

Fig.9 Effects of Young's modulus attenuation on ground response curve. (Parameter value: Set 1 – Hard rock, $v=v_r=0.2$, $\sigma_c^{Peak} = \sigma_c^R$ = 300MPa, $\beta_r=3.0$), (a) $\lambda=0.7$, $\theta=0°$; (b) $\lambda=1.1$, $\theta=90°$

5. Optimization support scheme for the circular tunnel under non-uniform pressure

Based on the above research, the state of surrounding rock shows the non-uniform change characteristic along its circumference under non-uniform pressure. When $0<\lambda<1$, the radius and deformation of the plastic zone show the change characteristics of the side wall > roof; and when $\lambda>1$, the result is on the contrary. Therefore, when the tunnel is excavated, the pressure of surrounding rock acting on the support bearing structure are not the same along the circumference. And then it is easy to cause the instability of the support structure due to local overload, so the traditional linear and equal strength support method cannot fully guarantee the overall stability of such tunnels, the non-linear dynamic support theory can provide an effective way to solve such problems. The principles of support design can be concluded in four parallel as follows [26]:

- Providing reinforced support to the key parts according to the fracture and deformation degree of the surrounding rock. Under the condition of non-uniform pressure, the range and surface displacement of the plastic zone show the non-uniform change characteristics around the tunnel. Therefore, the deformation and loosening pressure acting on the supporting structure are different, which can easily cause the support structure to be overloaded and instability. When $0<\lambda<1$, the key support part is in the side wall and when $\lambda>1$, it is at the roof and floor.

- Grouting reinforcement to improve the residual strength of fractured rock mass. The worse the quality grade of the rock mass is, the greater will be the influence of the burial depth, the dilatancy and the LPC on the surface displacement. Therefore, the deformation of surrounding rock can be reduced by grouting reinforcement. Meanwhile, based on the results of this paper, the parameters of the grouting will be optimized.

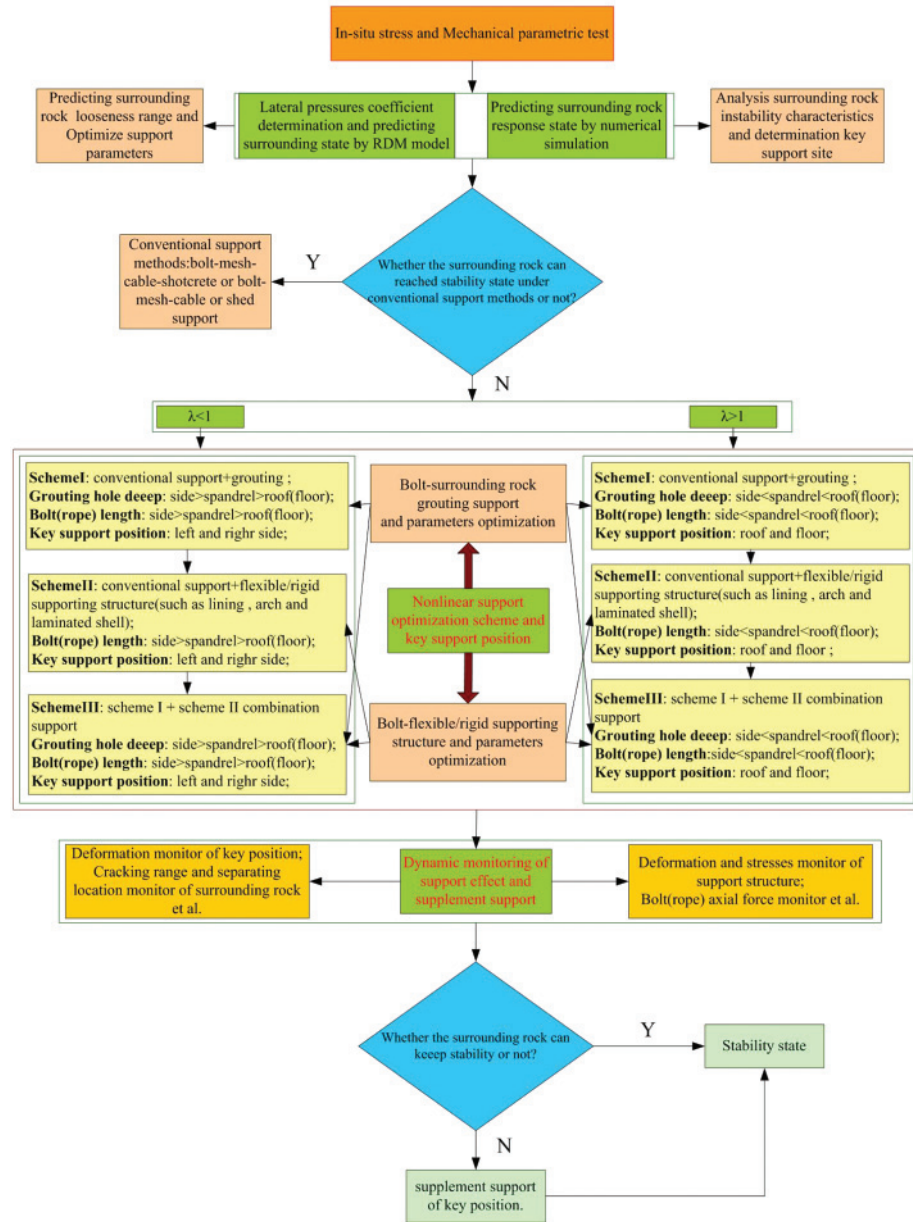- The strength and stiffness of the support structure

Fig.10 Optimization support scheme of deep circular opening under non-uniform pressure

should be coordinated with the deformation of the surrounding rock. And the key parts of the surrounding rock should be using a flexible support structure to moderate pressure or providing reinforced support.

- Dynamic monitoring of the support effect. Timely and dynamic monitoring of the stress and deformation of the surrounding rock can not only provide an important basis for evaluating the stability and reliability of the surrounding rock, but also provide practical bases for the further optimization of the support scheme.

According to the non-linear dynamic support theory, many support techniques of deep tunnel are put forward under non-uniform pressure, such as bolt-grouting support,

bolt-grouting - flexible arch combined support, bolt-mesh-cable and bolt-grouting combined support. Combined with the results of this study, the optimized method of the deep circular tunnel for support design under non-uniform pressure is summarized as shown in Fig.10.

6. Conclusion

Based on non-linear H-B criterion, a new approximate closed solution for the stress, deformation and plastic zone radius of the surrounding rock of the circular tunnel was established by considering the influence of the LPC and the Young's modulus attenuation. In order to reflect the influence of the damage on the deformation and ground response curve, three different Young's modulus attenuation models are considered. In addition, the influence of the LPC, dilatancy coefficient, buried depth and Young's modulus attenuation on the surrounding rock state is studied systematically. Finally, non-linear dynamic support design method under non-uniform pressure is proposed. The following conclusions can be drawn:

(1) A new approximate closed solution of a circular tunnel with non-uniform pressure is established by considering the influence of the dilatancy coefficient and damage. Compared to the Park's solution under uniform pressure, the correctness of this paper is verified.

(2) The LPC has a significant effect on the range and surface displacement of the plastic zone. With the increasing LPC, the range and surface displacement of the plastic zone in the side wall gradually decreases, while that in the roof and floor increases. Besides, when $0 < \lambda < 1$, the range and surface displacement of the plastic zone in the side wall are larger than those in the roof or floor. When $\lambda > 1$, the results are on the contrary.

(3) The LPC has an important influence on the ground response curve. With the increasing LPC, the maximum value position of the ground response curve is gradually transferred from the side walls (0º) to the roof (90º), whose changes will affect the determination of optimal support time as well.

(4) The dilatancy coefficient and burial depth have an important influence on the deformation of the surrounding rock, especially more significant for the poor quality grade rock mass. With the increasing dilatancy coefficient and burial depth, the surface displacement of surrounding rock gradually increases, too. Therefore, their effects on deformation of surrounding rock should be taken a full account of the support design.

(5) The effect of Young's modulus attenuation on the deformation of the plastic zone and ground response curve are not only related to the selection of the Young's modulus attenuation model, but also closely related to the spatial location and LPC of surrounding rock. Ignoring the continuity of Young's modulus attenuation, the deformation of surrounding rock is easy to be overestimated or underestimated. So, the Young's modulus power function attenuation seems to give more reasonable results.

(6) A non-linear dynamic support design method of the circular tunnel under non-uniform pressure is proposed, which can provide important theoretical bases for similar engineering support problems.

Conflicts of interest

The authors declare that there are no conflicts of interest regarding the publication of this paper.

Acknowledgments

References

1. Savin, G.N. (1961): Stress concentration around holes.(Gros, E (translator)). Oxford, UK: Pergamon.

2. Detournay, E & Fairhurst, C. (1987): Two-dimensional elastoplastic analysis of a long cylindrical cavity under non-hydrostatic loading. *Int. J. Rock Mech. Min. Sci.*, 24(4), 197-221.

3. Zhou Y, Lu A.Z, Kuang. L. (2013): Elastoplastic analysis on circle tunnels surrounding rock under Asymmetry load. *Advanced Materials Research*,Vols. 671-374, pp: 1091-1101.

4. Zhou. H, Kong. G.Q. (2016): A semi-analytical solution for cylindrical cavity expansion in elatic-perfectly plastic soil under biaxial in situ stress field.,1-12.

5. Zhao H. Z., Wang W. M., Wang L. (2013): Response models of weakly consolidated soft rock roadway under different interior pressures considering dilatancy effect. *J. Cent. South Univ*., (20): 3736-3744.

6. Hoek E, Brown ET. (1980): Empirical strength criterion for rock masses [J]. *Journal of Geotechnical and Geoenvironmental Engineering, ASCE*., 106(9): 1013-1035.

7. Hoek E, Brown ET. (1980): Underground excavations in rock. London: Institution of Mining and Metallurgy.

8. Sharan, S.K. (2008): "Analytical solutions for stresses and displacements around a circular opening in a generalized Hoek–Brown rock." *Int. J. Rock Mech. Min. Sci.*, 45, 78-85.

9. Carranza-Torres, C., Fairhurst, C. (2000): "Application of convergence-confinement method of tunnel design to rock masses that satisfy the Hoek-Brown failure. "Tunnel. *Undergr. Space Technol.*, 15 (2), 187-213.

10. Sharan, S.K. (2005): Exact and approximate solutions

for displacements around circular openings in elastic-brittle-plastic Hoek-Brown rock. *Int. J. Rock Mech. Min. Sci.*, 42, 542-549.

11. Park, K.H., Tontavanich, B., Lee, J.G. (2008): "A simple procedure for ground response curve of circular tunnel in elastic-strain softening rock masses." Tunnel. *Undergr. Space Technol.*, 23, 151-159.

12. Park, K.H., Kim, Y.J. (2006): "Analytical solution for a circular opening in an elastic-brittle-plastic rock." *Int. J. Rock Mech. Min.* Sci., 43, 616-622.

13. Lee, Y.K., Pietruszczak, S. (2008): "A new numerical procedure for elasto-plastic analysis of a circular opening excavated in a strain-softening rock mass." Tunnel. *Undergr. Space Technol.*, 23, 588-99.

14. Wang, S.L., Yin, X.T., Tang, H., et al. (2010): "A new approach for analyzing circular tunnel in strain-softening rock masses." *Int. J. Rock Mech. Min. Sci.*, 47, 170-178.

15. Chen, Ran., Tonon, F. (2011): "Closed-form solutions for a circular tunnel in elastic-brittle-plastic ground with the original and generalized Hoek-Brown failure criteria." *Rock. Mech. Rock. Eng.*, 44, 169-178.

16. Carranza-Torres C. (2004): Elasto-plastic solution of tunnel problem using the generalized form of the Hoek-Brown failure criterion. *Int. J. Rock Mech. Min. Sci.* Abstr., 41(3):480-1

17. Verman, M.; Singh, B.; Viladkar, M.N.; Jethwa, J.L. (1997): Effect of tunnel depth on modulus of deformation of rock mass. *Rock Mech. Rock Eng.,* 30, 121-127.

18. Asef, M.R.; Reddish, D.J. (2002): The impact of confining stress on the rock mass deformation modulus. *Geotechnique.*, 52, 235–241.

19. Brown, E.T.; Bray, J.W.; Santarelli, F.J. (1989): Influence of stress-dependent elastic moduli on stresses and strains around axisymmetric boreholes. *Rock Mech. Rock Eng.*, 22, 189-203.

20. Zhang. Q, Jiang B.S, Wu X.S, Zhang. H.Q, Han L.J. (2012): Elasto-plastic coupling analysis of circular openings in elasto-brittle-plastic rock mass[J]. *Theoretical and Applied Fracture Mechanics,* 60: 60-67.

21. Nawrocki, P.A.; Dusseault, M.B.(1995): Modelling of damaged zones around openings using radius-dependent Young's modulus. *Rock Mech. Rock Eng.*, 28, 227-239.

22. Chen, X.; Tan, C.P.; Haberfield, C.M. (1999): Solutions for the deformations and stability of elastoplastic hollow cylinders subjected to boundary pressures. *Int. J. Numer. Anal. Meth.* Geomech., 23, 779-800.

23. Zhang, C.G.; Zhao, J.H.; Zhang Q.H, Hu, X.D. (2012): A new closed-form solution for circular openings modeled by the Unified Strength Theory and radius-dependent Young's modulus. *Comput. Geotech.*, 42, 118-128.

24. Ewy, R.T.; Cook, N.G.W. (1990): Deformation and fracture around cylindrical openings in rock- I. Observations and analysis of deformations. *Int. J. Rock Mech. Min. Sci.* Abstr., 27, 387-407.

25. Xu, Z.L. (2010): Elasticity, 4th ed.; Higher Education Press: Beijing, China, pp. 75-76; ISBN 978-7-04-020213-7.

26. He, M.C.; Lu, X.J.; Jing, H.H. (2002): Characters of surrounding rock mass in deep engineering and its non-liner displacement-mechanical design concept. *Chin. J. Rock Mech. Eng.,* 21, 1215-1224.

27. Zhao Z.H., Wang W.M., and Wang L, (2013): "Response models of weakly consolidated soft rock roadway under different interior pressures considering dilatancy effect," *Journal of Central South University,* vol. 20, no. 12, pp. 3736-3744.